A New Look at Quasar Accretion Disks

Author(s):
Capellupo, Daniel M.; Netzer, Hagai; Lira, Paulina; Trakhtenbrot, Benny; Mejía, Julián

Publication date:
2013

Permanent link:
https://doi.org/10.3929/ethz-b-000422975

Originally published in:
IAU Symposium 9(S304), https://doi.org/10.1017/S1743921314004013

Multiwavelength AGN Surveys and Studies
Proceedings IAU Symposium No. 304, 2013
A. M. Mickaelian & D. B. Sanders, eds.

doi:10.1017/S1743921314004013

A New Look at Quasar Accretion Disks

Daniel M. Capellupo[1], Hagai Netzer[1], Paulina Lira[2], Benny Trakhtenbrot[3] and Julián Mejía[2]

[1]School of Physics and Astronomy, Tel Aviv University, Tel Aviv 69978, Israel
email: danielc@wise.tau.ac.il

[2]Departamento de Astronomía, Universidad de Chile, Camino del Observatorio 1515, Santiago, Chile

[3]Institute for Astronomy, Dept. of Physics, ETH Zurich, Wolfgang-Pauli-Strasse 27, CH-8093 Zurich, Switzerland

Abstract. The physics of active black holes (BHs) is governed by three key parameters: their mass, spin, and accretion rate. Understanding the cosmic evolution of these parameters is crucial for tracing back the growth of the BHs to the epoch of their formation. We have selected a unique AGN sample, in a narrow redshift range around z = 1.55, based on both BH mass and Eddington ratio, and we observed them with the X-Shooter instrument on the VLT, covering the rest wavelength range ∼1200 to 9800 Å. This wide wavelength range allows us to study, simultaneously, more emission lines (i.e., CIV 1550 Å through H-alpha), and a larger portion of the global AGN SED, than any previous studies. We currently have a sample of 30 quasars already observed and spanning BH masses from $\sim 10^8$ to 10^9 M_{solar} and Eddington ratio from ∼0.03 to 0.7. We focus here on our first science goal, comparing the observed AGN SED to thin accretion disk models in order to identify the origin of the SED. We also discuss the unique capability of this sample to identify any emission-line profile dependencies on BH mass and the Eddington ratio, and to compare mass determination methods based on four different emission-line profiles (Hα, Hβ, MgII 2800 Å, and CIV 1550 Å).

Keywords. quasars: general, accretion, accretion disks

1. Introduction

The physics of active black holes (BHs) is governed by three key parameters: their mass (M_{BH}), spin (a), and accretion rate ($\dot{M}$). To test how these parameters determine the observable attributes of AGN, we have selected a sample based on both M_{BH} and the Eddington ratio (L/L_{Edd}), which serves as a proxy for $\dot{M}$. Using the X-Shooter instrument on the VLT, we have obtained single-epoch, multi-wavelength spectra of 30 quasars with M_{BH} ranging from $\sim 10^8$ to $5\text{x}10^9$ M_{solar} and L/L_{Edd} from ∼0.03 to 0.7, with the aim of comparing various quasar properties with these key parameters. We are currently obtaining spectra for approximately 10 more quasars from X-Shooter, within this same redshift range, to extend our sample to smaller values of M_{BH} and L/L_{Edd}.

The X-Shooter instrument has three arms, covering three different wavelength regions, each with its own optimized optics, dispersive element, and detector. The three arms together cover the wavelengths 3000 to 25000 Å, continuously, with resolution ranging from 3300 to 5400. At the redshift of our sample, this corresponds to a wavelength range of ∼1200 to 9800 Å in the quasar rest-frame.

There are three main issues we want to address with this unique sample. The first is the origin of the AGN SED. A basic model used to describe the shape of the AGN SED is a geometrically thin, optically thick accretion disk, similar to the one described

in Shakura & Sunyaev (1973), and more recently in Davis & Laor (2011), and references therein. However, "slim" or "thick" accretion disks have also been considered, and there is evidence, from models, of such systems at larger values of L/L_{Edd} ($>\sim$0.3; e.g., Abramowicz *et al.* (1988), Ohsuga & Mineshige (2011), and Netzer (2013), and references therein). This has not been observationally confirmed thus far. Using our unique sample selection and uniquely wide wavelength coverage, we can put constraints on the origin of the observed AGN SED and how this origin changes depending on M_{BH} and L/L_{Edd}.

The other fundamental issue that we will be able to explore with our data is the physics of the observed broad emission lines (BELs) in type-I quasar spectra. The wide wavelength coverage of X-Shooter, and our chosen redshift range of z $\sim 1.45 - 1.65$, provides us with single-epoch coverage of the Hα, Hβ, MgII 2800 Å, and CIV 1550 Å emission lines. The observed BEL profiles are probably shaped by the BH gravity, the radiation pressure force, and the gas distribution in the BEL region. Our X-Shooter spectra, which cover many lines simultaneously and are thus not affected by source variability, provide the ideal sample for testing whether there is a correlation between emission-line profiles and M_{BH} or L/L_{Edd}. Finally, our sample provides a unique benchmark to compare M_{BH} estimates and their dependancy on the emission-line profiles of Hα, Hβ, MgII 2800 Å, and CIV 1550 Å. With single-epoch spectra that cover all of these emission lines for our entire sample, we can identify the most reliable methods and whether the mass determinations depend on the accretion disk and/or BH properties.

2. Origin of the AGN SED

Given the wide wavelength coverage of our data, we have a good constraint on the shape of the underlying continuum SED. We compare the shape of this observed SED to the expected SED from a thin accretion disk (AD) model. To produce this model, we use a numerical code described in Slone & Netzer (2012). This code is based on the Shakura & Sunyaev (1973) model of a geometrically thin, optically thick accretion disk, with a fixed viscosity parameter, α, and a spin-dependent innermost stable circular orbit, which determines the mass-to-energy conversion efficiency, η. The Slone & Netzer (2012) model includes comptonization of the emitted radiation in the AD atmosphere and general relativistic corrections.

The first part of our analysis is to identify whether the shape of the SED of each quasar can be fit by a thin AD model. Besides the aforementioned viscosity parameter, the main input parameters for the model is the SMBH mass (M_{BH}), the mass accretion rate ($\dot{M}$), the black hole spin (a), and the inclination of the disk. For each quasar, we calculate both M_{BH} and $\dot{M}$ directly from the observed spectrum. For M_{BH}, we use the FWHM of the MgII emission line, the luminosity at 3000 Å, and relations given in Trakhtenbrot & Netzer (2012). For $\dot{M}$, we use the value we obtained for M_{BH} from the MgII line, the luminosity at 8600 Å, and Eqn. 1 in Netzer & Trakhtenbrot (2013). We assume a face-on inclination for all the models.

We then run the AD model for each quasar with the calculated M_{BH} and $\dot{M}$, varying only the spin (a). For 14 out of 28 quasars, the thin AD spectrum provides a very good fit to the observed continuum SED (the observed spectra are corrected for Galactic extinction). For 7 out of 28, the fit is marginal, and for the remaining 7, there is no value of a that produces a fit to the observed spectrum. In Figure 1, we show an example of a quasar spectrum that is very well fit by the thin AD model, and an example where the thin AD model clearly does not fit the observed SED.

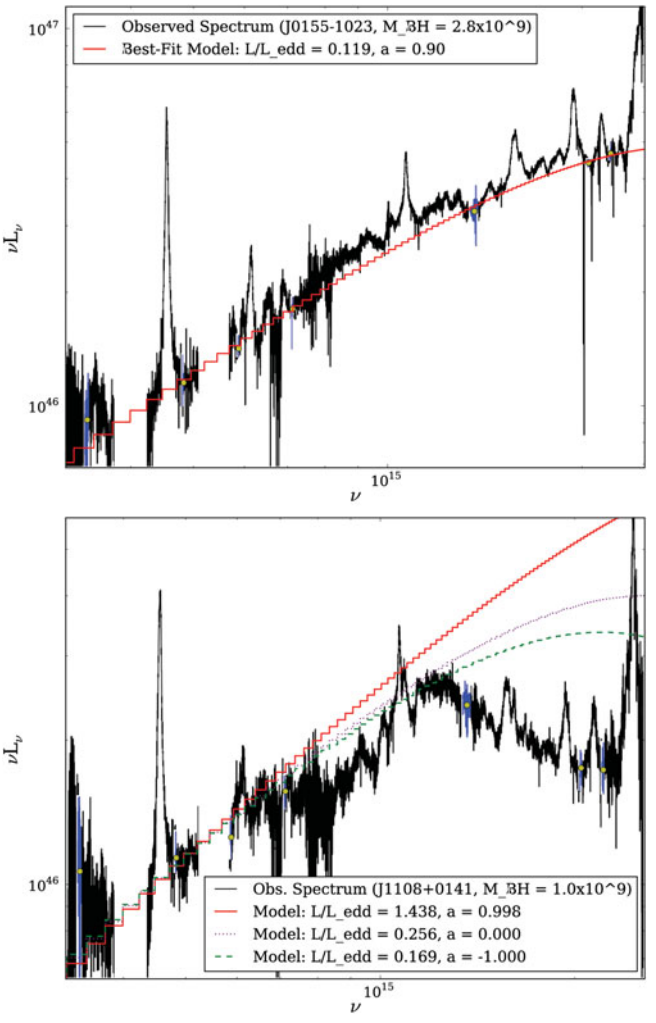

Figure 1. The top panel is an example of one of the 14 (out of 28) quasars where a thin AD model provides a good fit to the observed SED. The red curve is the best-fit model, and the continuum regions used for finding the best-fit model are shown in blue. The bottom panel is one of the 7 quasars which clearly are not fit by a thin AD model. In these quasars, even for models with a BH spin of -1, which have the lowest mass-to-energy conversion efficiency, the thin AD model overestimates the luminosity at shorter wavelengths.

Our preliminary results so far suggest that those quasars that we are not able to fit with a thin AD model all have high values of L/L_{Edd}, which may be related to the presence of a slim AD. This question is still under investigation.

3. BEL Profiles and Comparing M_{BH} Determination Methods

The wide wavelength coverage from X-Shooter allows us to compare the profiles and intensities of some of the most well-studied BELs (Hα, Hβ, MgII, and CIV) within a single-epoch spectrum. The procedure we follow is either to use the AD SED to fit the continuum, in cases where this provides good fits to local, line-free "windows" on the blue and red side of the line in question, or else fit a local power-law underneath the line.

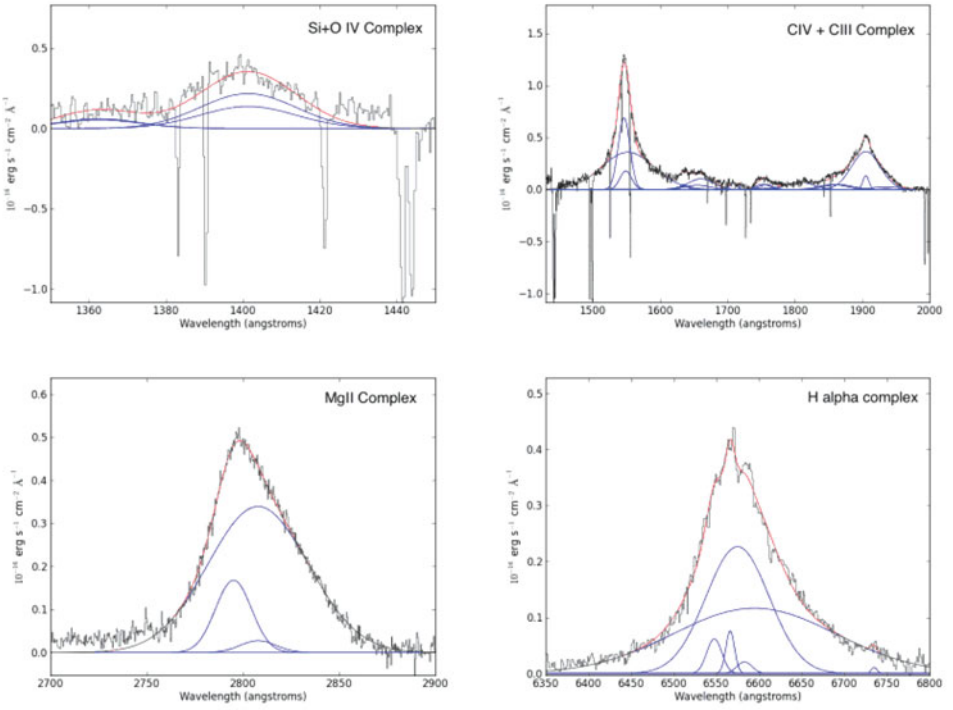

Figure 2. The red curves show the overall fit to some of the BELs our data covers. The blue curves show the individual Gaussians that contribute to the overall fit. This enlarged view of the BELs also illustrates the data quality we obtain from X-Shooter over the entire wavelength coverage.

A power-law fit to the entire spectrum does not provide a good fit to the continuum. We then fit the Balmer continuum emission and the global UV FeII emission (from 1950 to 3080 Å), using an FeII emission template.

After subtracting the continuum, we fit each BEL using multiple Gaussians. Figure 2 shows example fits for some of the main BELs. With these fits to the emission line profiles, we can compare the profiles and line intensities to other quasar properties.

The other primary science goal is to compare all of the main virial M_{BH} determination methods with our sample, which spans a wide range of M_{BH} and L/L_{Edd}. Given that we will have good profile measurements for Hα, Hβ, MgII, and CIV, we will likely be able to answer the question of which emission line, and under what conditions, provides the best estimate of M_{BH}.

References

Abramowicz, M. A., Czerny, B., Lasota, J. P., & Szuszkiewicz, E. 1988, *ApJ*, 332, 646
Davis, S. W. & Laor, A. 2011, *ApJ*, 728, 98
Netzer, H. 2013, *The Physics and Evolution of Active Galactic Nuclei*, 2013
Netzer, H. & Trakhtenbrot, B. 2013, arXiv:1311.4215
Ohsuga, K. & Mineshige, S. 2011, *ApJ*, 736, 2
Shakura, N. I. & Sunyaev, R. A. 1973, *A&A*, 24, 337
Slone, O. & Netzer, H. 2012, *MNRAS*, 426, 656
Trakhtenbrot, B. & Netzer, H. 2012, *MNRAS*, 427, 3081